JOURNAL OF AIRCRAFT
Vol. 29, No. 5, Sept.-Oct. 1992

Drag Computation by Vortex Methods

Mayer Humi*
Worcester Polytechnic Institute, Worcester, Massachusetts 01609

The vortex method in two dimensions is applied to compute the drag coefficients for flat and concave plates near zero angle of attack. We show numerically that near this angle the drag undergoes a bifurcation due to the symmetry breaking. An extension to the vortex algorithm which takes into account viscous effects outside the wall region is developed, and its results are compared with those of the $k = \epsilon$ model.

Nomenclature

e_z = unit vector in z direction
u = fluid velocity field
x_i = position of ith vortex
Γ = circulation
δ = Dirac δ function
δ_σ = "Blob" function approximating δ
ν = kinematic viscosity
ω = vorticity

I. Introduction

THE computation of the drag coefficient in various geometries is one of the important goals of numerical simulations in fluid dynamics.[1-3] These computations are especially crucial to the optimal design of decelerators.[4-9] The modeling of these structures must take into account dynamic shape deformations, but computer speeds at the present time permit the computation of the drag coefficient only for a structure of fixed shape. Computations to this end were performed in the past using the "SALE" algorithm[4] and some "flavors" of the vortex method in two dimensions.[10-14] However the SALE package does not use any turbulence model,[10] and therefore its results are meaningful only in the laminar region. To go beyond this region an appropriate turbulence model such as the k-ε model[10,15] or the vortex method must be used. In these later methods viscosity away from the wall region is usually neglected and various strategies (including some boundary-layer models) are used to satisfy the boundary conditions on the wall in conjunction with the creation of new vortices.[14] However a correct implementation of the viscosity effects outside the wall region appeared recently in the literature.[13]

The prime objective in this paper is to apply vortex methods in two dimensions to the accurate computation of the drag coefficient in various geometries. To this end two different implementations of the vortex methods are used. The first is due to P. Spalart[14] while the second is an extension of the first, taking into account viscosity effects outside the wall region. These results are compared with those of the k-ε model using the FLUENT package.[15] As a byproduct of these computations, a bifurcation is identified (numerically) in the value of the drag coefficient for geometries with reflection symmetry near zero angle of attack. This bifurcation is related to the symmetry breaking at these angles.

Sec. II describes briefly the vortex method and the algorithm used to implement the viscous effects away from the wall region. In Sec. III the results of the simulations are described with some conclusions.

II. Vortex Methods with Viscosity

Incompressible fluid flow is governed by Navier-Stokes equation

$$\nabla \cdot \boldsymbol{u} = 0 \tag{1}$$

$$\frac{\partial \boldsymbol{u}}{\partial t} + (\boldsymbol{u} \cdot \nabla)\boldsymbol{u} = -\nabla p + \nu \nabla^2 \boldsymbol{u} \tag{2}$$

The vorticity of the flow is defined as

$$\omega = \nabla \times \boldsymbol{u} \tag{3}$$

By taking the curl of Eq. (2) we obtain

$$\frac{\partial \omega}{\partial t} + (\boldsymbol{u} \cdot \nabla)\omega = \omega \cdot \nabla \boldsymbol{u} + \nu \nabla^2 \omega \tag{4}$$

For two-dimensional flows (we consider only this case in the following) $\omega \cdot \nabla \boldsymbol{u} = 0$ and Eq. (3) reduces to

$$\frac{\partial \omega}{\partial t} + (\boldsymbol{u} \cdot \nabla)\omega = \nu \nabla^2 \omega. \tag{5}$$

We observe that if ω is known then $\boldsymbol{u}$ can be computed using the Biot-Savart law. Thus

$$\boldsymbol{u}(x) = \frac{1}{2\pi} \boldsymbol{e}_z \times \int \frac{x - x'}{|x - x'|^2} \omega(x) \, dx' \tag{6}$$

The essence of the inviscid-vortex method[11,12] is to replace ω by

$$\omega(x) = \Sigma \Gamma_i \delta_\sigma (x - x_i) \tag{7}$$

where δ_σ are (blob) functions approximating the Dirac δ-function and Γ_i is the circulation of the ith vortex. The equations of motion of the individual vortices are given by [using Eq. (5)]

$$\frac{d\Gamma_i}{dt} = 0, \qquad \frac{dx_i}{dt} = \boldsymbol{u}(x_i, t) \tag{8}$$

The boundary conditions on a wall are satisfied in this algorithm by a variety of mechanisms[11,14] that couple these conditions to the creation of new vortices and the merger of old ones. Program KPD12 which was developed by NASA[14] contains such an implementation of the vortex method. We used

Received Nov. 15, 1990; revision received July 10, 1991; accepted for publication Aug. 14, 1991.

*Professor of Mathematics, Mathematical Sciences Department, 100 Institute Road.

this program with appropriate modifications to simulate flows around solid geometry.

The modifications in the code of KPD12 were as follows:

This program was used on a SUN workstation (vs CRAY in the original version). Accordingly double precision arithmetic was used whenever warranted.

The solution of a large linear system of equations is needed (at each time step) in this program to determine the circulation of the new vortices and the pressure gradient around the solid walls. The coefficient matrix of this system is not (very) ill conditioned, in general, but to improve accuracy a Gauss elimination with pivoting and scaling was implemented in the program.

The original program uses Head's method[16,17] to predict the separation point of the flow. The original implementation, however, uses Simpson's integration to solve the appropriate differential equation. This was replaced by a Runge-Kutta algorithm. To a large extent this stabilized the computation of the separation point.

In the second stage of the research the original code was modified to include viscous effects away from the wall. This was carried out in a spirit similar to Reference 13.

Replacing ω in Eq. (5) by its convolution with δ_σ leads to

$$\frac{d}{dt}[\omega^*\delta_\sigma(x)] = \nu\nabla^2(\omega^*\delta_\sigma) = \nu\nabla^2\delta_\sigma{}^*\omega \tag{9}$$

Discretizing ω as

$$\omega = \sum \Gamma_i\delta(x - x_i) \tag{10}$$

and substituting in Eq. (9) leads after proper integrations to

$$\sum \frac{d\Gamma_i}{dt}\delta_\sigma(x_j - x_i) = \nu \sum \Gamma_i\nabla^2\delta_\sigma(x - x_i) \tag{11}$$

Multiplying both sides of this equation by $\delta(x - x_j)$ and integrating yields

$$\sum_i \frac{d\Gamma_i}{dt}\delta_\sigma(x_j - x_i) = \nu \sum_i \Gamma_i\nabla^2\delta_\sigma(x_j - x_i) \tag{12}$$

Eq. (12) represents a system of coupled equations for the evolution of Γ_i. However as the number of vortices is large (~1300) it is not practical to solve this system in this form. To obtain a valid approximation observe that δ_σ are fast decreasing functions, and therefore the off-diagonal elements in the left-hand side of Eq. (12) are usually small. A reasonable approximation to Eq. (12) is given by

$$\delta_\sigma(0)\frac{d\Gamma_i}{dt} = \nu \sum_i \Gamma_j\nabla^2\delta_\sigma(x_j - x_i) \tag{13}$$

In the program

$$\delta_\sigma(x) = \frac{\sigma^2}{\pi(x^2 + \sigma^2)^2} \tag{14}$$

with $\delta^2 = 5.76.10^{-6}$. This justifies the approximation made in deriving Eq. (13).

III. Results

The flows around three thin-wall geometries which are related to parachutes were simulated in this project. These are shown in Figs. 1–3. Starting from potential flow its evolution was followed for 3000 iterations with time step of 5.10^{-3} and approximately 1300 vortices. Zero angle of attack was used, and the Reynold's number varied from 10^4 to 10^6. From these simulations the drag coefficient was obtained as an average over its value from the 1000th to the 3000th iteration. These average coefficients are plotted in Fig. 4 for inviscid fluid flow outside the wall region. The oscillations in the value of the drag coefficient with time are shown (for a representative case) in Fig. 5.

To gauge the impact of the viscous effects outside the wall region on the drag the algorithm presented in Sec. II was implemented and the drag coefficient reevaluated for the flat plate geometry (Fig. 1). The results of these simulations show that the approximation Eq. (13) is justified only for Reynold's number over 5.10^5. For lower Reynold's numbers the algorithm became unstable, and the resulting drag coefficient was incorrect.

The drag coefficient was evaluated also through a finite difference scheme with 35 × 75 grid (using FLUENT) with and without turbulence (using the k-ε model). The results of

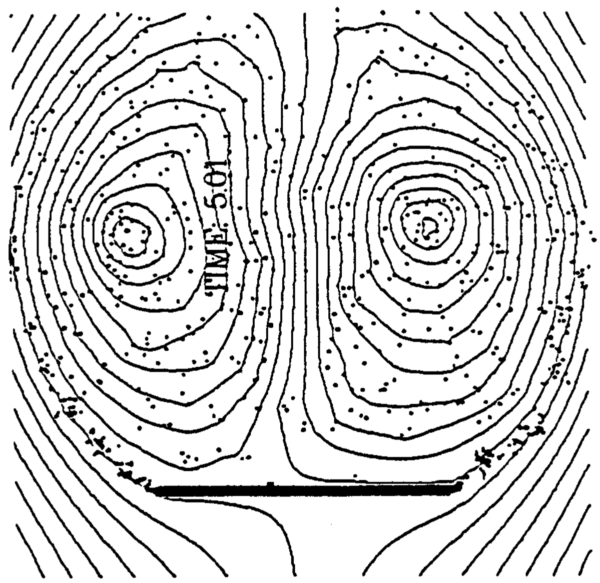

Fig. 1 Typical flow around flat plate at zero angle of attack. *Re* = 5.10^5.

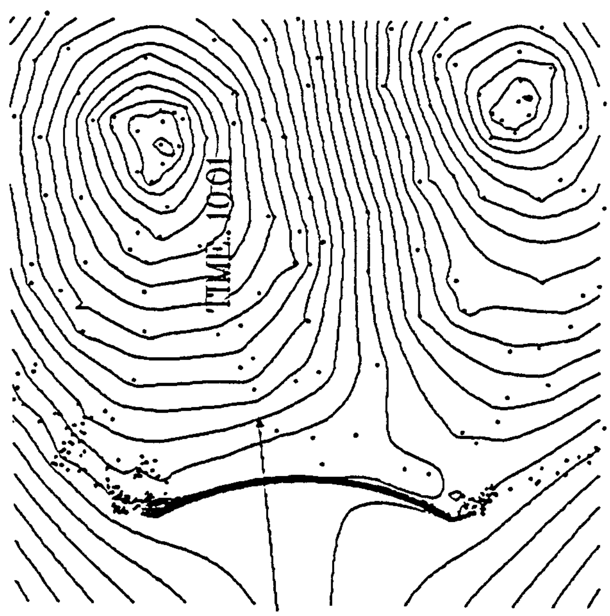

Fig. 2 Typical flow around a spherically concave plate.

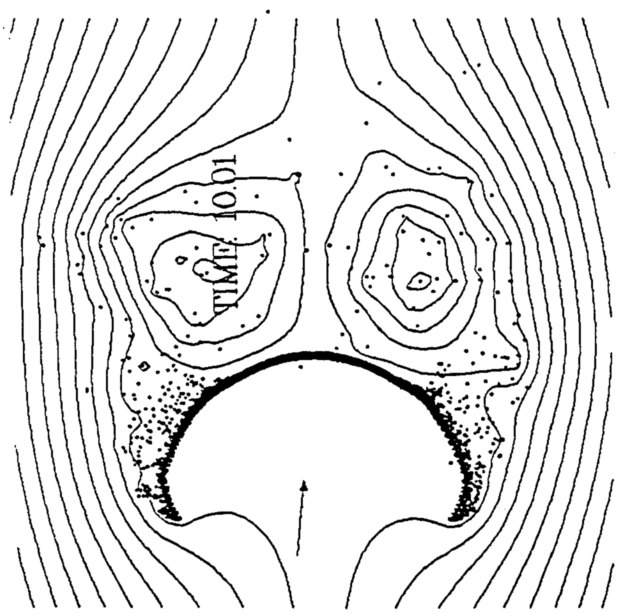

Fig. 3 Typical flow around a parachute-like structure.

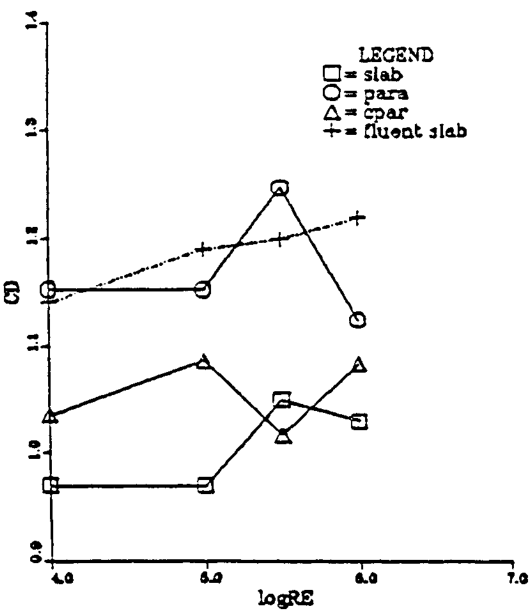

Fig. 4 CD vs Re for various geometries.

Table 1 Reynolds number

	10^4	10^5	5.10^5	10^6	10^7
Vortex-inviscid	0.97	0.97	1.02	0.93	0.94
Vortex-viscous	(2.4)	(3.1)	1.41	1.10	0.99
FLUENT-laminar	1.04	1.06	1.06	1.06	N/A
FLUENT-k-ε	1.20	1.22	1.22	1.22	N/A

these simulations are summarized in Table 1. The entries in this table show the impact of viscous effects outside the wall region and turbulence on the value of the drag coefficient. They also demonstrate the difference between several numerical schemes for the computation of this coefficient.

Simulations with nonzero attack angle were carried for flat plate geometry (Fig. 6). They show clearly the existence of a bifurcation in the value of the drag coefficient as the attack angle θ vary from zero. This bifurcation is due to the breaking of the reflection symmetry which exists when $\theta = 0$. The

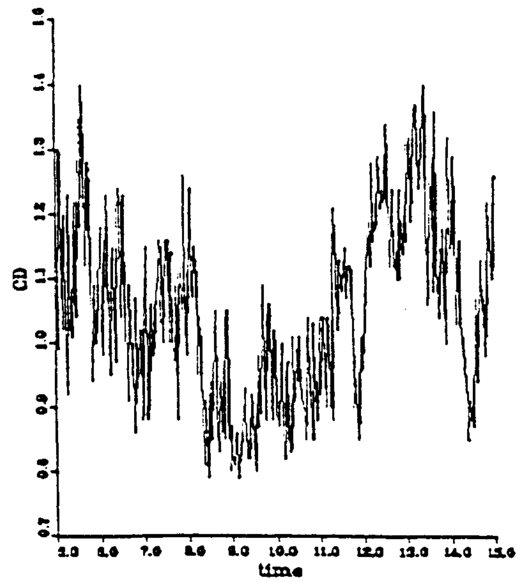

Fig. 5 Plate: CD vs time $Re = 5.10^5$.

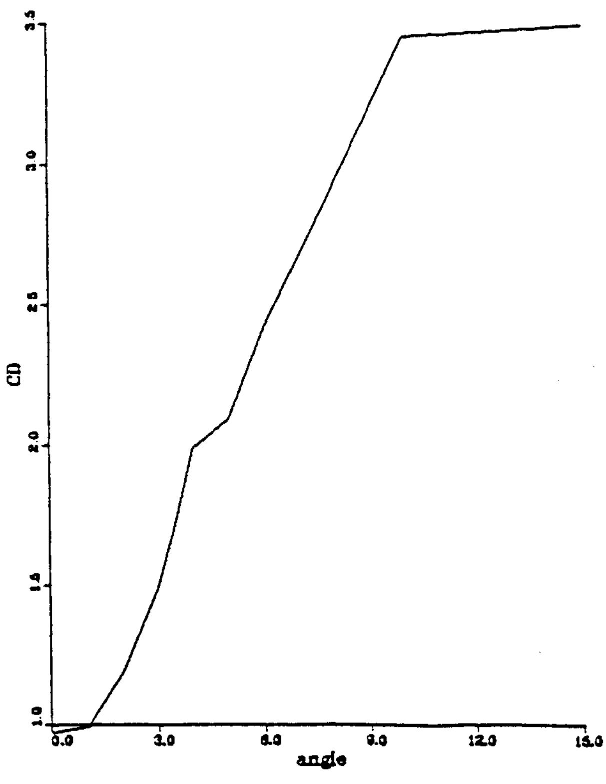

Fig. 6 Plate: CD vs angle $Re = 5.10^5$.

resulting drag coefficient (as a function of θ) and a typical flow pattern for $\theta = 6^0$ are shown in Figs. 6 and 7, respectively.

These computations demonstrate that the vortex method provides a robust algorithm for the calculation of the drag coefficient in two dimensions. The scheme suggested in these paper for the incorporation of viscous effects away from the wall led to improved drag coefficients at high Reynold's numbers which are consistent with those obtained from the k-ε model. Further research is needed to obtain a better understanding of the bifurcation in the drag coefficient for nonzero attack angles. A three-dimensional implementation of the vortex method is being developed at the present time. This will allow us to extend the present computations to more realistic structures.

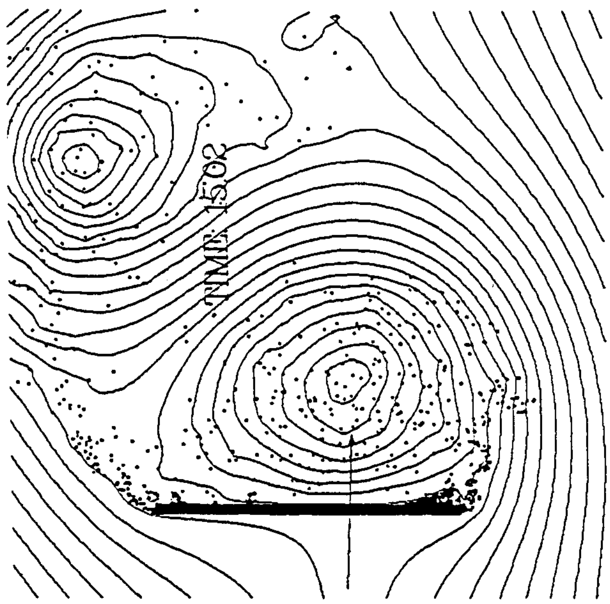

Fig. 7 Typical flow around flat plate. Angle of attack = 6 deg.

Acknowledgments

Part of this research was carried out at the Army Research Lab in Natick, MA. The author thanks E. C. Steeves for his kind help and encouragement.

References

[1]Dennis, D. R., "Recent Advances in Parachute Technology," *Aeronautical Journal*, Nov. 1983, p. 333–342.

[2]Pepper, W. B., and Maydew, R. C., Aerodynamic Decelerators—An Engineering Review," *Journal of Aircraft*, Vol. 8, 1971, pp. 1–11.

[3]Cockrell, D. J., The Aerodynamics of Parachutes," *AGARDOGRAPH*, No. 295, 1987.

[4]Steeves, E. C., "Analysis of Decelerators in Motion Using Computational Fluid Dynamics," AIAA Paper 89-0931, *AIAA 10th Aerodynamic Decelerator System Technology Conference*, Cocoa Beach, FL, 1989, pp. 269–278.

[5]Strickland, J., "A Vortex Panel Analysis of Circular Arc Bluff Bodies in Unsteady Flow," AIAA Paper 89-0929, *AIAA 10th Aerodynamic Decelerator System Technology Conference*, Cocoa Beach, FL, 1989, pp. 86–90.

[6]Higuci, H., and Park, O. W., "Computations of the Flow Past Solid and Slotted Two-Dimensional Bluff Bodies with Vortex Tracing Method," AIAA Paper 89-0930, *AIAA 10th Aerodynamic Decelerator System Technology Conference*, Cocoa Beach, FL 1989, pp. 90–96.

[7]Ibrahim, S. K., Potential Flow Field and Added Mass of Idealized Hemispherical Parachute, *Journal of Aircraft*, Vol. 4, 1967, pp. 96–100.

[8]Lee, C. K., Modeling of Parachute Opening, *Journal of Aircraft* 1989, pp. 444–451.

[9]Mayer, J., and Purvis, J. W., "Vortex Lattice Theory Applied to Parachute Canopy Configurations," *AIAA-84-0795 Proceedings of the AIAA 8th Aerodynamic Decelerator and Balloon Technology Conference*, Hyannis, FL, April 1984.

[10]Markatos, N. C., The Mathematical Modeling of Turbulent Flows, *Applied Mathematical Modeling*, 1986, pp. 190–236.

[11]Leonard, A., Computing Three Dimensional Incompressible Flow with Vortex Elements, *Annual Review of Fluid Mechanics*, Vol. 17, 1985, pp. 523–564.

[12]Chorin, A. J., Vortex Sheet Approximation of Boundary Layers, *Journal of Computational Physics*, Vol. 27, 1978, pp. 428–436.

[13]Fishelov, D., A New Vortex Scheme for Viscous Flows, *Journal of Computational Physics*, Vol. 86, 1990, pp. 211–224.

[14]Spalart, P. R., Vortex Methods for Separated Flows, NASA TM 100068. Numerical Simulation of Separated Flows, NASA TM 84328.

[15]Hutchings, B., and Iannuzzelli, R., Fluid Dynamics Software, *Mechanical Engineering*, July 1987, p. 60, Fluent is a product of Crearex Co., Hanover, NH.

[16]Head, M. R., Entrainment in the Turbulent Boundary Layers Aeronautical Research Council (Great Britain) Reports and Memoranda 3152, 1958.

[17]Cibeci, T., and Bradshaw, P., *Momentum Transfer in Boundary Layers*, McGraw-Hill, New York, 1977.